

Performance Analysis for Various Fiber-Optic CDMA Receiver structures

Sina Zahedi, Jawad A. Salehi

Department of Electrical Engineering
Sharif University of Technology, Tehran, 11365-9363, Iran
Advanced/Wideband CDMA Laboratory
Iran Telecom Research Center, Tehran, 13155-3961, Iran
szahedi@stanford.edu and jasalehi@sina.sharif.ac.ir

Abstract—In this paper we compare various receiver structures for Optical CDMA networks. Optical Orthogonal Codes (OOC) are utilized as signature sequences and the performance studied in this paper takes into account the effect of all major noise sources. Required mean number of photon count per chip time for reliable transmission of data bits for various receiver structures is investigated. Two general classes of receivers are investigated which use chip-time or bit-time electronic integration. The results show that receivers with chip-time integration have superior performance and therefore low-power transmission is possible at low speeds. However, the high-speed systems need bit-time integration and therefore should operate at higher levels of signal power.

I. INTRODUCTION

In recent years, there has been a tendency toward the use of spread spectrum techniques in fiber-optic multiple-access networks. This is mainly because of vast available bandwidth in fiber-optic lines. A spread spectrum system can use this excess bandwidth as processing gain to provide multiple access capability to the network. A spread spectrum multi-access system, was proposed in [1] using Optical Orthogonal Codes (OOC) as spreading codes for OOK incoherent optical signals. OOC is not the only viable candidate for Optical CDMA and other sequences such as prime sequences can be used as spreading sequences in a positive incoherent system. However, off-chip auto and cross-correlation properties of OOC which simplifies synchronization has made OOC as the preferred spreading sequence in asynchronous Optical CDMA systems. Performance analysis of such systems with various receiver structures was the subject of many articles [2], [5]–[8]. In this paper, we present a unified model for performance analysis of different proposed receiver structures taking into account all major noise sources, i.e., quantum shot-noise, photodetector dark current noise and circuit Gaussian noise. Our analysis is based on photon-counting techniques, which is proved to give the best BER predictions. For numerical computation of results, we avoid the common Gaussian approximations. However, since there are large numbers of effective parameters in BER (such as noise and interference terms), numerical calculation of bit error probability is quite intractable. For that reason, we use Saddle-Point approximation techniques for BER evaluation of these systems, which relies on characteristic function of the received decision criteria.

Section 2 of this paper gives a description of proposed CDMA system using OOC codes and introduces different

receiver structures. In section 3, we present BER analysis of different receiver structures and section 4 uses the saddle-point approximation technique for numerical evaluation of BER and presents the numerical results and conclusions.

II: FIBER-OPTIC CDMA NETWORKS

Fig. 1 shows a typical structure of a fiber-optic CDMA network. Each information source provides an information bit for a laser based optical OOK modulator every T second. Pulses generated by optical OOK modulator have duration $T_c = T/F$ where F is CDMA code length or processing gain of the system.

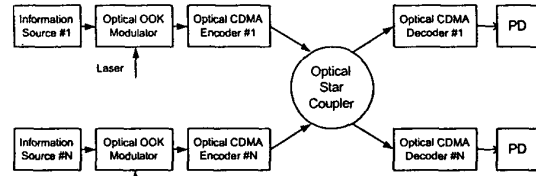


Fig. 1. Structure of Optical CDMA Networks

In optical CDMA encoder, energy of pulses generated by data modulator splits into K (Code Weight) equal parts where each part undergoes a pre-specified delay and recombine in such a way to form the CDMA code pattern at the output of CDMA encoder. We assume that OOC codes with minimum auto and cross-correlation is assigned to each user's encoder [1]. We denote by N , the number of active users of the network and by N_{\max} the maximum number of allowed users. Under conditions of minimum auto and cross-correlation, N_{\max} is limited to $(F - 1) / K(K - 1)$ [1].

At the receiver, a copy of the desired signal along with interference from all other $N - 1$ active users will be received, and the receiver should be able to decide which bit of the desired user has been sent. BER performance of the receiver is highly affected by architecture of CDMA decoder. Fig. 2 shows eight different receiver structures for fiber-optic based CDMA using OOC. In what follows for the remaining of this section, we will consider different receiver structures proposed for fiber-optic CDMA. The receiver structures studied here include structures with a number of simple electronic processing modules. Although, other receiver structures which use extensive

electronic signal processing such as pattern recognition or multi-user detection can be considered here, however, the required processing in electronic domain for the above mentioned receiver structures would not be desirable when one considers high-speed optical networks.

A. Passive Correlation Receiver [2]:

In this receiver, received signal will be compared against transmitter signature sequence. The whole receiver performs match filtering on the input signal. Incoming signal will be divided into K equal parts each undergoing a time delay complement to one of delay elements of CDMA encoder to form a filter inversely matched to the transmitted signature sequence. Output of these K delay lines will be combined and after photodetection and integration, output voltage will be sampled at the end of each bit interval. The sampled value, which is the output voltage of an integrator, will be compared against a threshold level Th and an estimation of the transmitted bit will be given.

B. Active Correlation Receiver [2]:

This receiver performs the same operation as passive correlation receiver. However, an active multiplier that can be implemented for example using an acousto-optic modulator will perform multiplication operation. Therefore, integration time after photodetector can be extended to T seconds and therefore this receiver has a simpler electronic design comparing with passive correlation receiver, but uses a more complicated optical technology.

C. Optical Hard-Limiter + Passive Correlator Receiver [2]:

This structure removes many interference patterns through using an optical hard-limiter before correlation receiver of Fig. (2.a). Optical Hard-Limiter at the input of correlator limits the energy of input pulses to the equivalent of one pulse thus considerably reduces the probability of a false alarm.

D. Optical Hard-Limiter + Active Correlator Receiver [2]:

This receiver uses a hard-limiter before active correlation receiver. Therefore, this structure needs a lower speed electronic technology.

E. Double Optical Hard-Limiter + Passive Correlation Receiver [7][9]:

Double optical hard-limiter structure removes many interference patterns, which will pass through a simple optical hard-limiter.

F. Double Optical Hard-Limiter + Double Correlation receiver [7][9]:

This structure is an alternate structure for receiver in Fig. 2.e where a lower speed electronic is required. It should be noted here that the proposed receiver structures in 2.e and

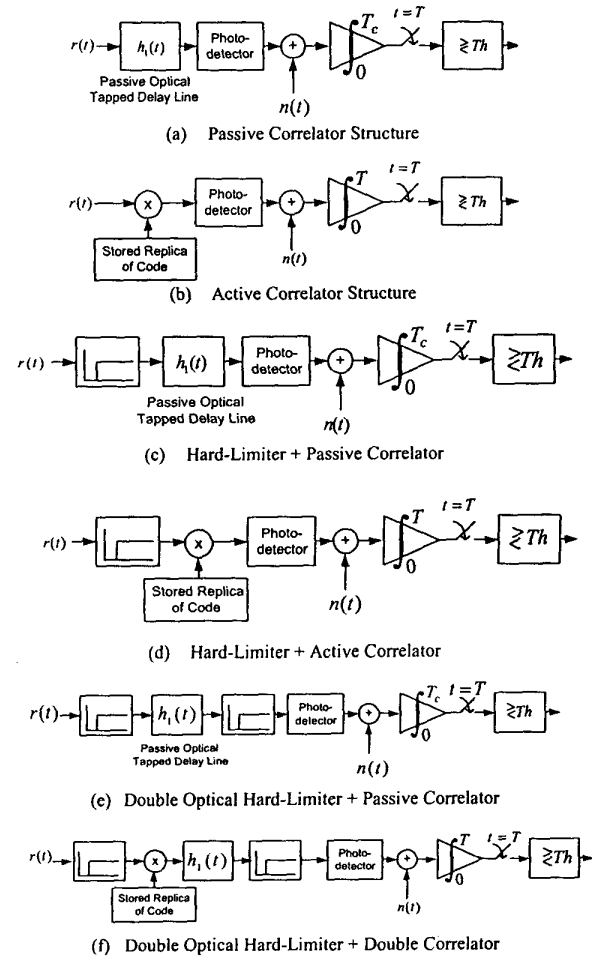
2.f are equivalent to the variations of an earlier proposed receiver structure based on ideal optical AND gates [9].

G. High-Speed Chip-Level Detector [6]:

Fig. 2.g shows the block diagram of a chip-level receiver. In this receiver, decision is based on K partial decision random variables. The received signal will be sampled at each chip pulse interval and a "1" bit will be detected when at least one pulse is present at all pulse positions and a single missed pulse at the designated code pulse position is sufficient to detect "zero" bit. It can be shown that if no noise is present, Hard-Limiter receiver performs as well as Chip-Level detector [6]. This receiver requires a fast electronic design.

H. Optical Chip-Level Detector [6]:

This is an alternate structure for receiver in Fig. 2.g that requires a lower speed electronic design. It should be noted that when there is no noise present, receiver structures (c)-(h) perform the same and their performances in multi-access limited conditions are limited to results in [2].



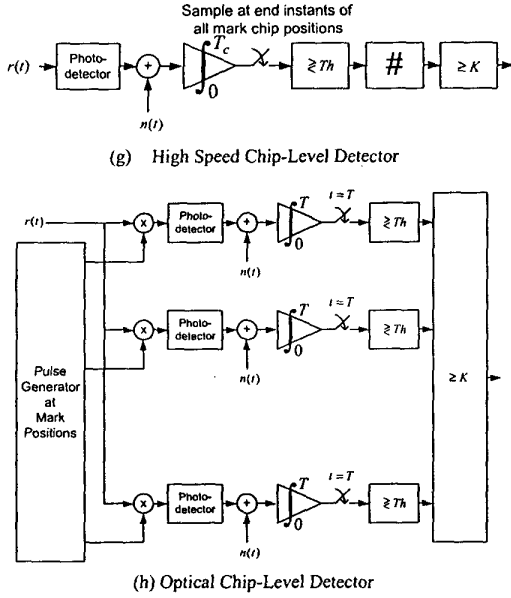


Fig. 2. Various Receiver Structures

III. BER PERFORMANCE ANALYSIS

In this analysis, we assume that different signals are frame asynchronous, i.e., no effort has been made to synchronize different transmitters. Analysis of BER of such a system seems quite intractable. A simplifying assumption is to consider different signals to be chip synchronous. This is a pessimistic case and gives an upper bound to the BER of the real asynchronous system [1].

We denote by $\alpha_j, j = 1, 2, \dots, K$ the number of interfering pulses received in j 'th pulse position and by $\vec{\alpha} = (\alpha_1, \alpha_2, \dots, \alpha_K)$ the vector of received interference. In OOC with minimum Auto and Cross-Correlation, two codewords cannot overlap at more than one pulse position. Since each code word has K pulses, there are K^2 ways of pairing the K pulses of two users. Therefore, the probability that two code words overlap at 1 pulse position is $q = K^2/2F$ where factor $1/2$ accounts for the probability that interfering user has sent "1". Assuming $N-1$ interfering users, the probability that there are l interfering pulses is given by

$$\Pr(l) = \binom{N-1}{l} q^l (1-q)^{N-1-l} \quad l = 0, 1, \dots, N-1 \quad (1)$$

Assuming l interfering pulses, there is a set of interference patterns so that $\sum_{i=1}^K \alpha_i = l$. We denote this set of vectors with F_l . Since l interfering users are distinguishable, they can produce K^l interference patterns. However, what is important for decision at receiver is vector $\vec{\alpha}$ not the specific users who have produced the interference pattern. Assuming l interfering pulses, pattern $\vec{\alpha}$ can be produced in

$$\binom{l}{\alpha_1, \alpha_2, \dots, \alpha_K} = \binom{l}{\alpha_1} \binom{l-\alpha_1}{\alpha_2} \dots \binom{\alpha_K}{\alpha_K} = \frac{l!}{\prod_{i=1}^K \alpha_i!} \quad (2)$$

ways each with probability $1/K^l$. Therefore, if $P_E(\vec{\alpha})$ is the probability of error given interference pattern $\vec{\alpha}$, then error probability can be expressed as:

$$P_E = \sum_{l=0}^{N-1} \Pr(l) P_E(F_l) \quad (3)$$

where from [5],

$$P_E(F_l) = \sum_{\vec{\alpha} \in F_l} \frac{l!}{K^l} \frac{P_E(\vec{\alpha})}{\prod_{i=1}^K \alpha_i!} \quad (4)$$

$P_E(\vec{\alpha})$ depends on receiver structure as well as interference pattern $\vec{\alpha}$. F_l is a set of $(l+K-1)!/(K-1)!$ vectors and generating and calculating their associated $P_E(\vec{\alpha})$ could be quite computationally intensive which makes the scheme impractical. We will find simplifying formulas for BER calculation depending on receiver structure. $P_E(\vec{\alpha})$ in each case not only depends on receiver structure, but also on photodetection parameters like signal power, noise power and photodetector quantum efficiency.

We assume that a reverse biased PIN diode is used as the photodetector. However, the analysis can be easily extended to estimate performance of other photodetector types such as Avalanche Photo Diode.

We assume that circuit noise has a power spectrum density $N_0(A^2/Hz)$. Therefore, if we integrate over a period of T seconds, variance of the output noise will be $\sigma^2 = N_0 T/2$ [3]. We denote by λ_d the dark current photoelectron rate of the photodetector. Therefore, mean of photoelectron count over a period of T seconds will be $\lambda_d T$. We also denote by λ_c the rate of photoelectron count due to a single chip pulse in receiver. λ_c depends on transmitter power, Code weight, receiver structure and quantum efficiency of the photodetector. We also assume that energy E_c is transmitted per OOK pulse. This energy will be divided into K equal parts in CDMA encoder and further will be divided into N_{max} equal parts in star coupler.

A. Passive Correlation Receiver

In this receiver, filter $h_i(t)$ is a set of passive optical tapped delay lines. Input pulses will be divided into K equal parts. Therefore, λ_c can be expressed as $\lambda_c = \eta E_c / (N_{max} K^2 T_c h f)$. In this receiver, $P_E(\vec{\alpha})$ depends on $\sum_{i=1}^K \alpha_i = l$ not just on the specific pattern $\vec{\alpha}$. Hence $P_E(F_l) = P_E(\vec{\alpha})$ and can be expressed as:

$$P_E(\vec{\alpha}) = \frac{1}{2} P_E(\vec{\alpha} | 0) + \frac{1}{2} P_E(\vec{\alpha} | 1) \\ = \frac{1}{2} \int_{-\infty}^{\infty} P_v(v | 0, \vec{\alpha}) dv + \frac{1}{2} \int_{-\infty}^{\infty} P_v(v | 1, \vec{\alpha}) dv \quad (5)$$

where

$$P_e(v|b, \bar{\alpha}) = \sum_{n=0}^{\infty} P(n|b, \bar{\alpha}) \left[\frac{\exp\left[-(v - e_0 n)^2 / 2\sigma^2\right]}{\sqrt{2\pi\sigma^2}} \right] \quad (6)$$

where b represents the transmitted bit and $\sigma^2 = N_0 T_c / 2$ and e_0 is the charge of electron. $P(n|b, \bar{\alpha})$ can be expressed as $P(n|b, \bar{\alpha}) = \text{Pos}(n, ((Kb+l)\lambda_c + \lambda_d)T_c)$ where $\text{Pos}(x, m) = e^{-m} m^x / x!$.

B. Active Correlation Receiver:

In this receiver, $\lambda_s = \eta E_s / N_{\max} K T_c h f$. Bit error rate of this receiver follows formulas (5) and (6) where $\sigma^2 = N_0 T / 2$ and $P(n|b, \bar{\alpha}) = \text{Pos}(n, (Kb+l)\lambda_c T_c + \lambda_d T)$.

C. Hard-Limiter + Passive Correlation Receiver:

In this receiver, number of non-zero elements of $\bar{\alpha}$ which we denote it by $|\bar{\alpha}|$ is the effective interference parameter. In other words $P_e(\alpha) = P_e(\beta)$ iff $|\bar{\alpha}| = |\bar{\beta}|$. Therefore, P_e can be expressed as:

$$P_e = \sum_{c=0}^K \Pr\{|\bar{\alpha}| = c\} P_e(\bar{\alpha}) \quad (7)$$

In appendix A, we have proved that:

$$\Pr\{|\bar{\alpha}| = c\} = \binom{K}{c} \sum_{i=0}^c (-1)^i \binom{c}{i} \left(1 - (K - c + i) \frac{K}{2F}\right)^{N-1} \quad (8)$$

In this receiver $\lambda_s = \eta E_s / N_{\max} K^2 T_c h f$ and optical hard-limiter clips the energy of pulses to $E_s / N_{\max} K$ and vanishes pulses with less energy. $P_e(\bar{\alpha})$ can again be expressed by (5) and (6) where $\sigma^2 = N_0 T_c / 2$ and $P(n|b, \bar{\alpha}) = \text{Pos}(n, \{(Kb + (1-b)c)\lambda_c + \lambda_d\}T_c)$.

D. Hard-Limiter + Active Correlation Receiver:

In this receiver $\lambda_s = \eta E_s / N_{\max} K T_c h f$ and optical hard-limiter clips the energy of pulses to $E_s / N_{\max} K$ and vanishes pulses with less energy. $P_e(\bar{\alpha})$ can again be expressed by (5) and (6) where $\sigma^2 = N_0 T / 2$ and $P(n|b, \bar{\alpha}) = \text{Pos}(n, (Kb + (1-b)c)\lambda_c T_c + \lambda_d T)$.

E. Double Optical Hard-Limiter + Passive Correlator Receiver:

In this case, error occurs when transmitted bit is "1" but receiver fails to detect the transmitted bit, because of quantum noise effects or circuit noise. The other case is that when transmitted bit is "0" and criteria passes the threshold value because of interfering users or dark current or circuit noise. Probability of error can be expressed by (5), (6), (7) and (8) where $\sigma^2 = N_0 T_c / 2$ and $\lambda_s = \eta E_s / N_{\max} K^2 T_c h f$ and $P(n|b, \bar{\alpha})$ can be expressed as

$$P(n|b, \bar{\alpha}) = \begin{cases} \text{Pos}(n, (K\lambda_c + \lambda_d)T_c) & (b=1) \text{ or } (b=0, c=K) \\ \text{Pos}(n, \lambda_d T_c) & (b=0, c < K) \end{cases}$$

F. Double Optical Hard-Limiter + Double Correlator Receiver:

In this receiver, $\lambda_s = \eta E_s / N_{\max} K^2 T_c h f$ and probability of bit error can be expressed by (5), (6), (7) and (8) where,

$$P(n|b, \bar{\alpha}) = \begin{cases} \text{Pos}(n, K\lambda_c T_c + \lambda_d T) & (b=1) \text{ or } (b=0, c=K) \\ \text{Pos}(n, \lambda_d T) & (b=0, c < K) \end{cases}$$

where $\sigma^2 = N_0 T / 2$.

G. High-Speed Chip-Level Detector:

In this receiver, $\lambda_s = \eta E_s / N_{\max} K T_c h f$. Output voltage of each integrator will be compared to a threshold voltage Th . We note that if $\bar{\alpha}$ and β are permutations of each other, then $P_e(\bar{\alpha}) = P_e(\beta)$. Therefore, in order to calculate $P_e(F_i)$, it is not necessary to generate all vectors in F_i . We define a new set G_i so that elements of G_i are non-increasing elements of F_i , i.e., $\bar{\alpha} \in G_i$ iff $\bar{\alpha} \in F_i$ and $\alpha_1 \geq \alpha_2 \geq \dots \geq \alpha_K \geq 0$. Number of permutations of vector $\bar{\alpha}$ can be expressed by $N(\bar{\alpha})$ where $N(\bar{\alpha}) = K! / \prod_i R(\alpha_i)!$, where $R(\alpha_i)$ is number of repetitions of α_i in $\bar{\alpha}$ and product is taken over i for which α_i are distinct. Therefore, $P_e(F_i)$ can be expressed as:

$$P_e(F_i) = \sum_{\bar{\alpha} \in G_i} \frac{N(\bar{\alpha}) P_e(\bar{\alpha})}{K! \prod_{i=1}^K \alpha_i!}$$

elements of G_i can be generated using recursive algorithms. $P_e(\bar{\alpha})$ can be calculated as follows:

$$\begin{aligned} P_e(\bar{\alpha}) &= \frac{1}{2} P_e(\bar{\alpha} | 0) + \frac{1}{2} P_e(\bar{\alpha} | 1) \\ &= \frac{1}{2} \prod_{i=1}^K \Pr(v_i \geq Th | \alpha_i, b=0) \\ &\quad + \frac{1}{2} \left(1 - \prod_{i=1}^K \Pr(v_i \geq Th | \alpha_i, b=1)\right) \end{aligned} \quad (9)$$

where v_i is the output of i 'th integrator and:

$$\Pr(v_i \geq Th | \alpha_i, b) = \sum_{n=0}^{\infty} P(n | \alpha_i, b) \left[\frac{\exp\left[-(v - e_0 n)^2 / 2\sigma^2\right]}{\sqrt{2\pi\sigma^2}} \right] \quad (10)$$

where $\sigma^2 = N_0 T_c / 2$ and $P(n|b, \alpha_i) = \text{Pos}(n, \{(b + \alpha_i)\lambda_c + \lambda_d\}T_c)$. It can be seen that $\Pr(v_i \geq Th | \alpha_i, b)$ is a function of $b + \alpha_i$ which ranges from zero to $N+1$. Therefore, it is sufficient to calculate all $N+2$ possible values of (10) once for each specific $\lambda_s, \lambda_d, \sigma$, store in an array and then use these pre-stored values to calculate (9).

H. Optical Chip-Level Detector:

In this receiver, $\lambda_s = \eta E_s / N_{\max} K^2 T_c h f$. $P_e(\bar{\alpha})$ can be expressed by (9) and (10) where $\sigma^2 = N_0 T / 2$ and $P(n|b, \alpha_i) = \text{Pos}(n, (b + \alpha_i)\lambda_c T_c + \lambda_d T)$.

IV. NUMERICAL RESULTS AND CONCLUSIONS

Numerical evaluation of equation (5) and (6) can be quite time consuming and needs high precision variables and calculation. Because of very small values of BER, calculation using ordinary variables can make erroneous results.

We have used saddle-point approximation method in order to compute the numerical values of these equations. In order to evaluate equation (5) using saddle-point approximation method, characteristic function of random variable v_i (accumulated charge in the integrator) should be evaluated. Conditioned on transmitted bit and interference pattern $\bar{\alpha}$, random variable v_i is the summation of a noise sample with variance σ^2 and the total charge of released photoelectrons. σ^2 is the variance of accumulated charge in the integrator due to circuit noise. Charge of each electron is e_0 and number of photoelectrons is a random variable with Poisson distribution. Therefore, characteristic function of compound random variable v_i assuming that number of photoelectrons N has a Poisson distribution with mean K_s can be expressed by $\Phi(s) = \phi_{v_i|b,\bar{\alpha}}(s) = E(e^{v_i s}) = e^{K_s(e^{e_0 s} - 1)} e^{s^2 \sigma^2 / 2}$. A new function $\psi(s)$ is defined where,

$$\psi(s) = \ln \frac{\Phi(s) e^{-Ths}}{s} = K_s (e^{e_0 s} - 1) + \frac{s^2 \sigma^2}{2} - Ths - \ln|s| \quad (11)$$

Positive and negative roots of equation $\psi'(s) = 0$ are called s_0 and s_1 , respectively. Saddle-Point approximation states that [4]:

$$\int_{-\infty}^{\infty} P_{v_i}(v|b,\bar{\alpha}) dv \approx \frac{\exp[\psi(s_0)]}{\sqrt{2\pi\psi''(s_0)}}, \quad \int_{-\infty}^{\infty} P_{v_i}(v|b,\bar{\alpha}) dv \approx \frac{\exp[\psi(s_1)]}{\sqrt{2\pi\psi''(s_1)}}$$

We assume a CDMA system with $R_b = 100 \text{ Mbps}$ per user and assume that OOC codes with code length $F = 2000$ and weight $K = 9$ with $N_{\max} = 27$ has been used. We also assume that photodetector dark current is $i_d = 160 \text{ nA}$ which is a typically high value for dark current noise. Therefore, mean dark current electron count in each chip time interval ($T_c = 5 \text{ ps}$) would be $m_d = 5$.

We assume that σ^2 is the variance of the thermal circuit noise added to the output of the receiver. For simplicity, we will use parameter $\sigma_n = \sigma/e_0$ which is the normalized value of standard deviation of additive Gaussian noise. The results of BER in each condition and for each structure of receiver have been derived for optimum threshold that its value is obtained by trial and error.

Performance degradation of receiver with structure of Fig. 2.a versus mean photon count per chip is shown in Fig. 3 for several values of σ_n . The base for performance degradation is quantum limit condition, i.e., no circuit and dark current noise. It can be seen that performance degradation due to circuit noise can be quite severe especially when the received signal is very low power.

Dependence of BER on mean photon count per chip is depicted in Fig. 4 for different receiver structures. We have assumed $\sigma_n = 30$ as a typical value. It can be seen that double optical hard-limiter or optical AND Gate BER approaches very fast to the ideal no noise BER. The effect of circuit noise on the performance degradation of chip-level receivers is quite severing. Structure of Fig. 2.h, which performs very well in quantum-limit conditions [6],

has a very poor performance when dark current noise and Gaussian circuit noise is considered.

Finally, the effect of number of simultaneous users on the performance of the system is shown in Fig. 5 for various receiver structures.

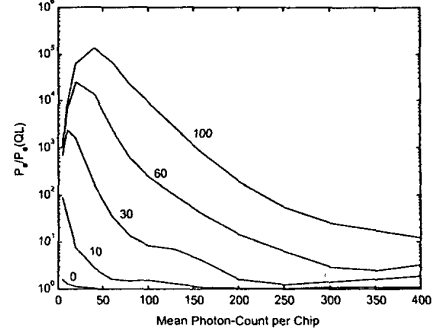


Fig. 3. Performance degradation of correlation receiver

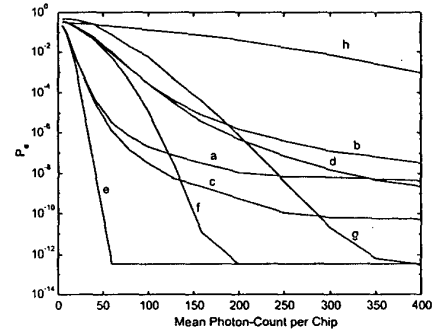


Fig. 4. dependence of BER on mean photon count per chip, $\sigma_n = 30$

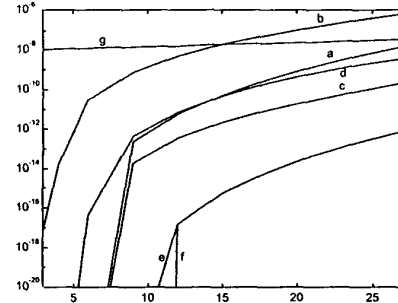


Fig. 5. dependence of BER on number of simultaneous users of the network, $\sigma_n = 30$

APPENDIX A

In this appendix, we prove equation (8). Translating this problem into the familiar problem of ball and box, we are confronted with this problem: We place l distinguishable balls into K equal boxes. $\Pr\{\bar{\alpha} = c | l\}$ is the probability that exactly c out of K boxes are filled. We will denote by $S(l, K, c)$ the number of ways that only c out of K

boxes are filled with l distinguishable balls. We know from [5] that $S(l, K, K)$ is on the form of:

$$S(l, K, K) = \sum_{i=0}^{K-1} (-1)^i \binom{K}{i} (K-i)^l$$

We note that $S(l, K, c) = \binom{K}{c} S(l, c, c)$. Therefore,

$$S(l, K, c) = \binom{K}{c} \sum_{i=0}^c (-1)^i \binom{c}{i} (c-i)^l$$

each of these $S(l, K, c)$ states have probability $1/K^l$. Therefore,

$$\begin{aligned} \Pr\{\bar{\alpha}|=c\} &= \sum_{i=0}^{N-1} \binom{N-1}{i} q^i (1-q)^{N-1-i} \frac{1}{K^l} \binom{K}{c} \sum_{i=0}^c (-1)^i \binom{c}{i} (c-i)^l \\ &= \sum_{i=0}^c \binom{K}{c} (-1)^i \binom{c}{i} \sum_{i=0}^{N-1} \binom{N-1}{i} q^i (1-q)^{N-1-i} \frac{1}{K^l} (c-i)^l \\ &= \binom{K}{c} \sum_{i=0}^c (-1)^i \binom{c}{i} \sum_{i=0}^{N-1} \binom{N-1}{i} \left(\frac{q}{K} (c-i) \right)^l (1-q)^{N-1-i} \\ &= \binom{K}{c} \sum_{i=0}^c (-1)^i \binom{c}{i} \left[1 - (K-c+i) \frac{K}{2F} \right]^{N-1} \end{aligned}$$

ACKNOWLEDGEMENTS

The authors would like to thank Dr. M. Nasiri-Kenari, M. Razavi and M. Abtahi for their helpful comments. We also thank Dr. M. Hakkak and Dr. M. Beik-Zadeh for support of this project. This work has been done as part of contract 7834330 with Iran Telecom Research Center (ITRC), Tehran, Iran.

REFERENCES

- [1] J.A. Salehi, "Code Division Multiple Access Techniques in Optical Fiber Networks - Part I: Fundamental Principles," *IEEE Trans. On Commun.*, vol. 37, no. 8, pp. 824-833, August, 1989
- [2] J.A. Salehi and C.A. Brackett, "Code Division Multiple Access Techniques in Optical Fiber Networks - Part II: System Performance analysis," *IEEE Trans. On Commun.*, vol. 37, no. 8, pp. 834-842, August, 1989
- [3] R.M. Gagliardi, S. Karp (1995), *Optical Communications*, Wiley, New York
- [4] C.W. Helstrom, "Approximate Evaluation of Detection Probabilities in Radar and Optical Communications," *IEEE Trans. Aerospace Electr. Syst.*, vol. AES-14, pp. 630-640, July, 1978
- [5] M. Azizoglu, J.A. Salehi and Y. Li, "Optical CDMA via Temporal Codes," *IEEE Trans. On Commun.*, vol. 40, no. 7, pp. 1162-1170, July, 1992
- [6] H.M.H Shalaby, "Chip-level detection in optical code-division multiple-access," *J. Lightwave Technol.*, vol. 16, pp. 1077-1087, June, 1998
- [7] T. Ohtsuki, "Performance analysis of direct-detection optical asynchronous CDMA systems with double-optical hard-limiters," *J. Lightwave Technol.*, vol. 15, pp. 452-457, Mar, 1997
- [8] H.M. Kwon, "Optical Orthogonal Code Division Multiple Access System-Part I: With Avalanche Photodiode Noise and Thermal Noise," *IEEE Trans. Commun.*, vol. 42, pp. 2470-2479, July, 1994
- [9] J.A. Salehi, "Emerging Code-Division Multiple Access Communications Systems," *IEEE Network Magazine*, vol. 3, no. 2, pp. 31-39, March, 1989